31st Annual International Conference of the IEEE EMBS
Minneapolis, Minnesota, USA, September 2-6, 2009

Intervention of Cardiomyocyte Death based on the Impedance-sensing Technique of Monitoring Cell Adhesion

Yiling Qiu, Ronglih Liao, and Xin Zhang, *Member, IEEE*

***Abstract*—Cardiomyocyte death is a critical risk factor in a variety of cardiovascular diseases [1, 2]. At the level of individual cardiomyocytes, cell adhesion alters at the early phase of ongoing death. It suggested the possibility of detecting the early sign of cell death through cell detachment and so that we could intervene in the cell response before cell fell into step with the irreversible death processes. In this work, we demonstrated the application of our impedance-sensing technique [3] in the intervention of cell responses to chemical stimuli. The results showed that the cell detachment could be detected with our impedance-sensing technique earlier than conventional biochemical staining techniques, and it could be used to guide the precautionary removal of TNF-α from the cell culture to intervene in the cell responses and prevent cardiomyocytes from cell death.**

I. Introduction

CARDIOMYOCYTE loss by cell death is significantly dangerous because it causes irreversible damage to adult hearts due to their very limited regeneration capability. Deregulated death of cardiomyocytes has been implicated as a fundamental patho-physiological mechanism in a variety of heart diseases, such as acute myocardial infraction, congestive heart failure or congenital heart diseases [1, 2].

There are two major processes of cell death which are apoptosis and necrosis. In the signaling pathways of cardiomyocyte apoptosis, caspases, the central executioners of apoptosis [4], mediate a series of cleavage of essential proteins, including focal adhesion kinase (FAK), at the early phase of the apoptosis. The inactivation of FAK causes immediate cell detachment from adjacent cells or ECM. Likewise, in cardiomyocyte necrosis, the rapture of cell membrane results in cell detachment. The capability to monitor the cell adhesion change noninvasively and in real time can be a potential technique for building up the sensing and regulation loop to intervene in ongoing cell death processes.

Electric cell-substrate impedance sensing (ECIS), first defined by Giaever, is a noninvasive and sensitive detecting technique for cell adhesion [5, 6], in which the impedance time course of cell-covered electrodes is recorded and attributed to various cell behaviors. In the last two decades, ECIS sensing has been employed to monitor many types of cells, including fibroblast, endothelial cells, cancer cells etc. [7-9]. More recently, ECIS research turned to excitable cells, such as skeletal muscle cells [10] and cardiomyocytes [11]. Generally, time courses of overall impedance during the biological processes were recorded in time intervals and attributed to various cell behaviors. To extract direct and detailed information from the overall signals, researchers [12, 13] further developed advanced data processing techniques. In these methods, morphological parameters, such as cell-substrate distance, are solved for precise description of cell adhesion [12, 14]. It has been reported that the ECIS method is capable of detecting vertical motion in the order of 1 nm [6]. Combining with other biophysical and biochemical assays, ECIS had been applied to study apoptosis of endothelial cells [15]. However, unlike endothelial cells or fibroblasts in the reported ECIS cases which exhibit known and constant electrical properties due to the reliable commercialized cell lines, cardiomyocytes are primarily cultured, which means unknown and unstable electrical properties have to be solved for each sample. In our preliminary research [3], a real-time monitoring technique has been developed on the basis of electrochemical impedance sensing (EIS) and electrical cell-substrate impedance sensing (ECIS). In this technique, equivalent cell-substrate distance is used to describe the extent of cell adhesion.

In this work, our impedance-sensing technique was employed to real-time monitor the cardiomyocyte culture. The response of cardiomyocytes to TNF-α was recorded in time courses of equivalent cell-substrate distance. The transition from cell adhesion to detachment was detected in the continuous treatment of TNF-α. TNF-α was removed from the cardiomyocyte culture as the intervention of cell responses before the critical moment of transition, which resulted in continuously enhancement of cell and adhesion and prompted cell survival.

II. Experimetal

A. Fabrication of the Impedance Sensor

The fabrication of the biosensing chips was conducted in a microfabrication laboratory. A glass slide was chosen as the substrate material because it could minimize the substrate capacitance and decrease the measurement noise. The electrode voids of the chips were patterned on the slides with

Manuscript received April 7, 2009. This work was supported in part by the U.S. National Science Foundation under Career Award (No. 0239163) and NER Award (No. 0609147).

Yiling Qiu is with Boston University, Boston, MA 02215 USA (e-mail: qiu@bu.edu)

Ronglih Liao, was with Boston University School of Medicine, Boston, MA 02118 USA. She is now with the Brigham and Women's Hospital, Harvard Medical School, Boston, MA 02115 USA (e-mail: rliao@rics.bwh.harvard.edu).

Xin Zhang is with the Department of Mechanical Engineering, Boston University, Boston, MA 02215 USA. (phone: 617-358-2702; fax: 617-353-5548; e-mail: xinz@bu.edu).

photoresist Shipley 1813 in photolithography on the MA6 aligner. The metal electrodes of biosensors were made of Cr (125Å) and Au (375Å) in a lift-off process. SiO_2 and SiN_x were deposited with magnetic sputtering to form an insulating layer with a thickness of 1200 Å, which was followed by an RIE process for exposure of the gold-coated electrodes. A biosensing chip consisted of 16 circular working electrodes (0.502 mm^2) and one common rectangular counter electrode (2.0 cm^2). Fig. 1a shows the configuration of the biosensing chip.

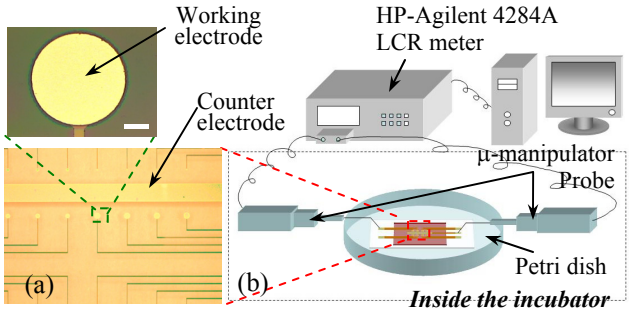

Figure 1: (a) Top view and close view of the counter and working electrodes. The scale bar is 200 μm. (b) Schematic diagram of the impedance measurement system. The part surrounded by dash lines is inside the incubator.

B. Testing System

The schematic diagram and photo of our impedance-sensing system is depicted in Fig. 1b. The biosensing chip was maintained in the incubator at 5% CO_2 and 37 ºC to avoid any fluctuations in the testing environment. Inside the incubator, the biosensing chip was mounted to a homemade silicone chamber designed for cell culture. The impedance of the electrodes in the chip was measured with an Agilent 4284A LCR meter (Agilent Technologies Inc., CA). The impedance measurement process was controlled by LabViewvirtual instruments.

C. Cardiomyocyte Isolation and Culture

Left ventricular (LV) myocytes were isolated from male Wistar rats according to a previously established protocol with some modifications [19]. The rat heart was separated and perfused with Ca^{2+}-free Krebs buffer (0.12 mol/L NaCl, 4.7 mmol/L KCl, 1.2 mmol/L KH_2PO_4, 1.2 mmol/L $MgSO_4$, 25 mol/L $NaHCO_3$, and 12 mmol/L glucose) and enzyme buffer (375 mg/L Collogenase and 425 mg/L Hyaluronidase in Ca^{2+}-free Krebs buffer). The rat heart was then cut into 8 to 10 small pieces and dispersed in enzyme buffer (Trysin 0.3 mg/mL and DNAase 0.3 mg/mL in Ca^{2+}-free Krebs buffer). The cardiomyocyte suspension was subsequently filtered through a nylon mesh, resulting in a typical yield of >90% rod-shaped cells. The isolated cells were then washed with DMEM, and were ready for plating onto microelectrodes. For the ECM, a laminin suspension was prepared by diluting the laminin solution (Becton-Dickinson) in serum-free medium at volume ratio of 1:100. The laminin suspension was dropped onto the impedance-sensing electrodes which were then kept still in the incubator for at least 30 min until a laminin layer formed. For electrical measurement, the biosensing chip was inoculated with 1.5 mL of the cardiomyocyte suspension, leading to a concentration of 5 × 10^4 cells per cm^2 of electrode area.

D. Impedance Spectroscopy

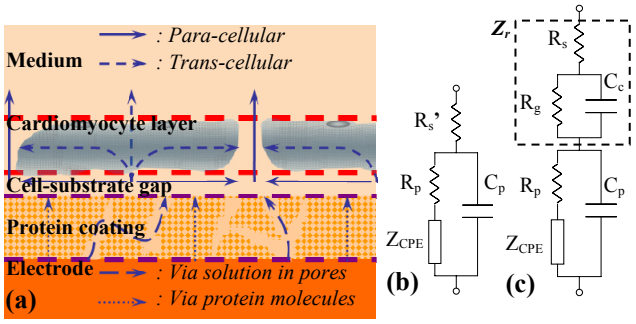

Figure 2: (a) Current flow patterns on the testing electrode. There are two modes of current in protein coating layer: one travels via solution in the pores among protein molecules; the other travels via protein molecules. There are also two modes of current in cardiomyocyte layer: Para-cellular mode represents how the current travels in solution around cells; trans-cellular mode represents how the current travels through the cell body. (b) Equivalent circuit model of impedance of the cell-free system (Z_n). (c) Equivalent circuit model of impedance of the cell-covered electrode (Z_c).

We measured impedance spectra with a 5mV voltage excitation in a wide frequency range from 20 Hz to 200 kHz, thus 80 testing frequencies were logarithmically evenly spaced to ensure the accuracy at low frequency. One round of frequency scanning was completed in 1 min. For the continuous monitoring, the cyclic frequency scanning was applied to the testing system every 10 min.

The equivalent circuit model of cell-free system was shown in Figure 2b where capacitor C_p and resistor R_p were used to represent the capacitance and resistance the porous laminin layer (schematic in Figure 2a). A constant phase element (CPE) was used to account for the nonlinearities of frequency-related electrical double layer impedance on the uncovered electrode surface ($Z_{CPE} = [Q_{CPE}(j\omega)^n]^{-1}$), where j and ω is the imaginary unit and angular frequency respectively). Resistor R_s' is the solution resistance. This model was fit and modified to the 3D impedance response plot in a complex nonlinear least square (CNLS) curve fitting program. The P weighting was added into the objective function of CNLS curve fitting to ensure the validity in case the fitting to the real and imaginary components were unbalanced.

The cell-related impedance (Z_r) was represented with three elements in the equivalent circuit model of cell-covered system (Figure 2c). C_c was used to represent the reactance of cells and R_g was used to describe the resistance of the thin medium layer in the cell-substrate gap. R_s was the resistance of bulk medium body. To achieve in the automation in determining the element parameters, the cell-related admittance response ($Y_r = Z_r^{-1}$) was first analyzed in a Nyquist plot. The electrical parameters acquired in the Nyquist plots of Y_r were utilized as the initial guess of the following CNLS curve fitting. Every loop in the cyclic frequency scanning went through the EIS data processing to determine R_g, R_s and C_c values.

In our methodology, a time course of equivalent cell-substrate distance was defined on the basis of a time course of normalized equivalent cell-substrate distance and an initial value of absolute cell-substrate distance [3]. Since R_g, the ion-conductive resistance, obeyed the Ohm's law, it would be reasonable to define the normalized equivalent cell-substrate distance was inversely proportional to the normalized R_g. The absolute cell-substrate distance was calculated with Lo's ECIS model of cell [13] in which the cell membrane impedance was considered as capacitive reactance ($Z_m = -j / (\omega C_c)$) and the cell-covered impedance (Z_c) was expressed with Z_m and Z_n. The absolute cell-substrate distance (h) was obtained in the ECIS calibration with Lo's model. When calibrated with the result of ECIS, the real time recording of normalized R_g could be translated into the time course of equivalent cell-substrate distance.

III. RESULTS AND DISCUSSION

A. Real-time Monitoring of Cell Death Induced by TNF-α

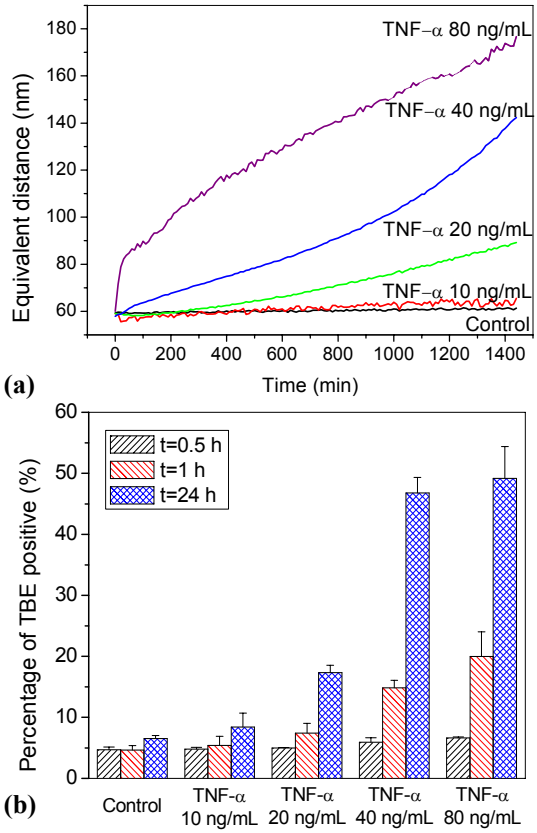

Figure 3: (a) Adhesion profiles of cardiomyocytes treated continuously with different concentration of TNF-α. (b) Percentage of death obtained with TBE tests in treated cardiomyocytes at t=0.5 h, t=1 h and t=24 h (n=3). Data from three independent experiments are shown in mean ± S.D.

The real-time monitoring was performed to cardiomyocytes treated with different concentrations of TNF-α and shown in cell adhesion profiles in Figure 2a. Though the initial equivalent distances were close, the samples treated with higher concentrations exhibited faster ascent than those with lower concentrations. Especially at the beginning stage of treatment, the 10 and 20 ng/mL samples experienced a drop in equivalent distance for about 2 h and then continuous ascent in slow rates. The cell detachment observed in our assay was related to the activation of TNF-α-induced cardiomyocyte death process. The TBE test was employed for the demonstration of cell death. After 30-minute treatment, even though no obvious difference could be found in the TBE results (Figure 2b), cell detachment was observed with our assay in the 40 and 80 ng/mL TNF-α-treated samples. The early detection of cell detachment provided us ongoing cell death information prior to TBE tests.

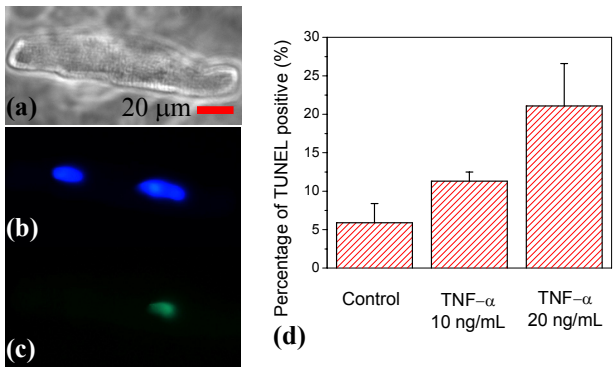

Figure 4: (a) Phase contrast image of the TNF-α-treated sample. (b) Corresponding fluorescent image of the DAPI-stained TNF-α-treated sample. (c) Corresponding fluorescent image of the TUNEL-stained TNF-α-treated sample. (d) Percentage of TUNEL-positive cardiomyocytes TNF-α-treated and control samples at t=24 h. Distinct difference was shown between the death percentages of TNF-α-treated samples and the control (n=3, P<0.01 for both concentration levels).

Since cardiomyocytes treated with 10 and 20 ng/mL TNF-α exhibited mild and slow cell detachment slopes, we considered apoptosis could be the major process of cell death. TUNEL tests (Figure 4) confirmed the apoptotic percentages of cardiomyocyte were close to the death percentages. Namely, the apoptosis was the major death mechanism in cardiomyocytes treated with 10 and 20 ng/mL TNF-α. TNF-α-induced apoptosis were executed by the caspases family which would break cell adhesion. However, our results showed that the cell detachment at these samples occurred after two-hour TNF-α treatment. It suggested the possibility of preventing cardiomyocyte apoptosis through removing TNF-α before the critical moment of cell detachment.

B. Intervention of Cardiomyocyte Responses to TNF-α

The instant reading of cell detachment also provided opportunities to intervene in the process of cell death. The short-term treatment of TNF-α was carried out at the concentration of 10 ng/mL. After 2 h, TNF-α-containing medium was replaced with serum-free medium. The treated cardiomyocyte layer was continuously monitored since the beginning of TNF-α treatment. As shown in Figure 5a, a rapid descent of cell-substrate distance occurred in the first 2 h of exposure, followed by a slow descent in the rest of 24-hour monitoring. The cell-substrate distance curve of

short-term treated cardiomyocytes showed a similar tendency with that of the long-term treated ones within the first 2 h, while the removal of TNF-α caused distinct tendencies afterwards. At the end of 24 h of monitoring, the TNF-α treated sample exhibited a significant decrease in cell-substrate distance while that of the control sample was a slight increase. Since the cell adhesion kept continuous enhancement in our experiments, the cardiomyocyte responses to TNF-α treatment was intervened in by the removal of TNF-α. As the result of intervention, the short-term treated cardiomyocytes also presented a low cell death percentage (5.8 ± 0.7 %) in the TBE test (Figure 5b) after a 24-hour incubation. Comparing with the death percentages of the control and the long-term treated cardiomyocytes, the short-term treatment with TNF- tended to be promotional for the cell survival rather than the cell death.

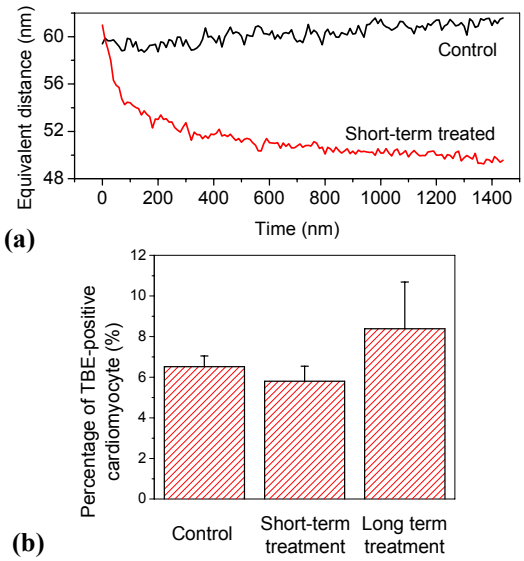

Figure 5: (a) Adhesion profiles of cardiomyocyte treated with 10 ng/mL TNF-α for 2 h. (b) TBE tests of short-term and long-term treated cardiomyocytes at t=24 h. Distinct difference was shown between the death percentages of the short-term and long-term treated samples (n=3, P<0.05).

IV. CONCLUSION

In this work, the intervention of ongoing cell death was achieved through the impedance-based detection technique and the corresponding removal of chemical stimuli. The cell adhesion of cardiomyocytes was real-time monitored and used as the criterion of cell responses to the external stimuli. Since cell detachment was one of the morphological evidences at early phases of apoptosis, intervention could be applied before the critical moment of cell detachment to prevent cardiomyocytes from ongoing cell death. The removal of TNF-α from the cardiomyocyte culture resulted in continuously strengthened cell adhesion with a promoted cell survival percentage. In the field of cell biology, this novel sensing and regulation technique is promising to become a high throughput experimental approach which will benefit from its non-invasiveness and convenience.

ACKNOWLEDGMENT

The authors would like to thank Xu Wang, Bo Wang, Jian Guan, Jianru Shi, Jian Guan, Michael Bauer and other colleagues at Cardiac Muscle Research Laboratory, Brigham and Women's Hospital, Harvard Medical School for their technical advice.

REFERENCES

[1] H. N. Sabbah, V. G. Sharov, and S. Goldstein, "Cell death, tissue hypoxia and the progression of heart failure," *Heart Fail Rev,* vol. 5, pp. 131-8, Jun 2000.

[2] A. Haunstetter and S. Izumo, "Apoptosis: Basic Mechanisms and Implications for Cardiovascular Disease," *Circulation Research,* vol. 82, pp. 1111-1129, 1998.

[3] Y. Qiu, R. Liao, and X. Zhang, "Real-time monitoring primary cardiomyocyte adhesion based on electrochemical impedance spectroscopy and electrical cell-substrate impedance sensing," *Anal Chem,* vol. 80, pp. 990-6, Feb 15 2008.

[4] M. O. Hengartner, "The biochemistry of apoptosis," *Nature,* vol. 407, pp. 770-6, Oct 12 2000.

[5] I. Giaever and C. R. Keese, "Monitoring fibroblast behavior in tissue culture with an applied electric field," *Proc Natl Acad Sci U S A,* vol. 81, pp. 3761-4, Jun 1984.

[6] I. Giaever and C. R. Keese, "A morphological biosensor for mammalian cells," *Nature,* vol. 366, pp. 591-2, Dec 9 1993.

[7] C. D. Xiao, B. Lachance, G. Sunahara, and J. H. T. Luong, "Assessment of cytotoxicity using electric cell-substrate impedance sensing: Concentration and time response function approach," *Anal Chem,* vol. 74, pp. 5748-5753, Nov 15 2002.

[8] J. H. T. Luong, M. Habibi-Rezaei, J. Meghrous, C. Xiao, K. B. Male, and A. Kamen, "Monitoring motility, spreading, and mortality of adherent insect cells using an impedance sensor. ," *Anal Chem,* vol. 73, pp. 1844-1848, 2001.

[9] S. Earley and G. E. Plopper, "Disruption of focal adhesion kinase slows transendothelial migration of AU-565 breast cancer cells," *Biochem Biophys Res Commun,* vol. 350, pp. 405-12, Nov 17 2006.

[10] V. Aas, S. Torbla, M. H. Andersen, J. Jensen, and A. C. Rustan, "Electrical stimulation improves insulin responses in a human skeletal muscle cell model of hyperglycemia," *Ann N Y Acad Sci,* vol. 967, pp. 506-15, Jun 2002.

[11] M. Yang, C. C. Lim, R. Liao, and X. Zhang, "A novel microfluidic impedance assay for monitoring endothelin-induced cardiomyocyte hypertrophy," *Biosens Bioelectron,* vol. 22, pp. 1688-1693, 2007.

[12] I. Giaever and C. R. Keese, "Micromotion of mammalian cells measured electrically," *Proc Natl Acad Sci U S A,* vol. 88, pp. 7896-900, Sep 1 1991.

[13] C. M. Lo and J. Ferrier, "Impedance analysis of fibroblastic cell layers measured by electric cell-substrate impedance sensing," *Physical Review E,* vol. 57, pp. 6982-6987, Jun 1998.

[14] C. M. Lo, C. R. Keese, and I. Giaever, "Impedance analysis of MDCK cells measured by electric cell-substrate impedance sensing," *Biophys J,* vol. 69, pp. 2800-7, Dec 1995.

[15] S. Arndt, J. Seebach, K. Psathaki, H. J. Galla, and J. Wegener, "Bioelectrical impedance assay to monitor changes in cell shape during apoptosis," *Biosens Bioelectron,* vol. 19, pp. 583-94, Jan 15 2004.

[16] C. C. Lim, M. H. Helmes, D. B. Sawyer, M. Jain, and R. Liao, "High-throughput assessment of calcium sensitivity in skinned cardiac myocytes," *Am J Physiol Heart Circ Physiol,* vol. 281, pp. H969-74, Aug 2001.